

# MULTISPECTRAL IMAGE CAPTURE USING TWO RGB CAMERAS

*Raju Shrestha and Jon Yngve Hardeberg*

The Norwegian Color Research Laboratory; Gjøvik University College, Norway  
 raju.shrestha@hig.no; jon.hardeberg@hig.no

## ABSTRACT

The development of faster and more cost effective acquisition systems is very important for the widespread use of multispectral imaging. This paper studies the feasibility of using two commercially available RGB cameras, each equipped with an optical filter, as a six channel multispectral image capture system. The main idea is to pick the best pair of filters from among readily available filters that modifies the sensitivities of the two cameras in such a way that their dominant wavelengths spread well spaced throughout the visible spectrum. Simulations with reasonably large number of available filters show encouraging result clearly indicating the possibility of using such systems.

## 1. INTRODUCTION

Acquisition is one of the important parts in the field of multispectral imaging. It is well known that with a panchromatic imaging sensor and three well-chosen optical filters, it is possible to obtain a fairly good reconstruction of the color tristimulus values of the reference human observer as defined in colorimetry. Multispectral image acquisition aims to estimate the spectral reflectances of the scene by using more than three filters.

There are currently three main approaches that are widely used in designing spectral-based digital camera systems:

1. *Narrow band image capture with a panchromatic sensor:* It involves the use of a panchromatic digital camera and narrow band sampling. Several methods can be used to achieve the narrow band sampling of the spectrum, including monochromator devices, liquid crystal tunable filters (LCTF), and narrow-band interference filters.
2. *Wide band image capture with a panchromatic sensor:* This approach typically uses a smaller set of wide band optical filters to capture digital image data and then uses spectral reconstruction algorithms to estimate the spectral reflectances of an object. This approach produces reasonable results because both man made and natural materials generally have smooth spectral reflectance shapes, thus the number of channels can be reduced to between eight and ten channels with broader band pass filters while still achieving accurate results. This approach is generally quite accurate spectrally, but acquisition is often quite slow, expensive, and special equipment is required. Image quality depends heavily on the camera.
3. *Wide band image capture with an off-the-shelf tri-chromatic digital camera:* This approach uses a high quality tri-chromatic digital camera in conjunction with spectral absorption filters to acquire unique spectral information [1, 2]. This method enables three channels of data to be captured per exposure as opposed to one. This greatly increases the speed of capture and allows the use

of technology that is readily available and does not need to be specialized. Such cameras are generally optimized to achieve good perceptual image quality. Still we have to take several shots with each chosen filter; this severely limits the usability for non-stationary scenes.

## 2. MULTISPECTRAL IMAGE CAPTURE WITH TWO RGB CAMERAS

This is the approach under our study in this paper. Here, instead of one, we use two normal digital (RGB) cameras. The idea is to select a pair of appropriate color filters, one for each camera, so that they will modify the sensitivities to give six reasonably well spaced channels in the visible spectrum. The subsequent combination of the images from of both cameras provides a six channel multispectral image of the objects in the acquired scene. Ohsawa et al. [3] discussed six band HDTV camera system which used beam splitter and interference filters. Our approach is much simpler with normal digital cameras and absorption filters which avoids angular dependency as with interference filters. We assume that the two cameras can be somehow arranged and aligned properly so that both cameras take the same areas of the object, or that this alignment is performed in a post-processing stage. One way to solve the alignment problem would be by setting up the two cameras in a stereoscopic configuration and then through the use of one or more stereo matching algorithms [4, 5, 6, 7]. Additional benefit of stereoscopic configuration is that it allows to acquire the 3D depth information as well. Thus, we can associate a reflectance spectrum with each 3D reconstructed point. Such a system could be used for many applications, for example for 3D artwork object acquisition. Knowing the spectral reflectance allows us to simulate the appearance of a 3D object under any virtual illuminant. Moreover, it lets us store this valuable information for future restoration.

The next section addresses an important question on how to best select the pair of filters from among a set of available filters.

## 3. SELECTION OF FILTERS

In our work, the filters are to be chosen from readily available filters in the market. A pair of filters, one each for two cameras is to be selected from them. Several filter selection algorithms have been proposed previously for color and multispectral imaging [8, 9, 10]. They are:

1. *Equi-spacing of filter dominant wavelength:* This is the first and most intuitive method where we simply try to find a combination of filters which spread the dominant wavelengths equally spaced across the spectrum of interest [8, 9]. But, it is not practicable for large combination of filters.

2. *Progressive optimal filters*: In this method, the  $k$ th filter is selected from the set of available filters as the one that shows the highest correlation to the progressive optimal filter of the first  $k$  characteristic reflectances (PCA analysis), having only positive values [8, 9].
3. *Maximizing filter orthogonality*: It chooses a set of filters whose non-normalized vectors have a maximized orthogonality [8, 9].
4. *Maximizing orthogonality in characteristic reflectance vector space*: Here, the idea is to select filters that have a high degree of orthogonality after projection into the vector space spanned by the  $r$  most significant characteristic reflectances [8, 9].
5. *Exhaustive Search*: All possible combinations of the filters is evaluated and the one that gives the best result is chosen. So it clearly gives the optimal solution [8, 9, 10]. However, the complexity of this method could be prohibitive, since it requires the evaluation of permutations.

In our study, as we have to choose just two filters from the set, the exhaustive search method is feasible and a logical choice because of its guaranteed optimal results. In order to reduce the computational complexity, infeasible filter pairs are excluded based on secondary criteria: Filter pairs that result in a maximum transmission factor of less than forty percent, and less than ten percent of the maximum transmission factor in one or more channels are excluded.

#### 4. EXPERIMENTAL SETUP AND RESULTS

The experiments are performed through simulation, with different pairs of real and imaginary camera pairs. Here, we are presenting two cases as illustrations. The simulation is carried out with the camera sensitivities, filters, and the test target defined spectrally.

1. *Camera Sensitivities*: The sensitivities of two commercial SLR cameras: Nikon D70, and Canon 20D, that are used in the experiment, are shown in the Figure 1.

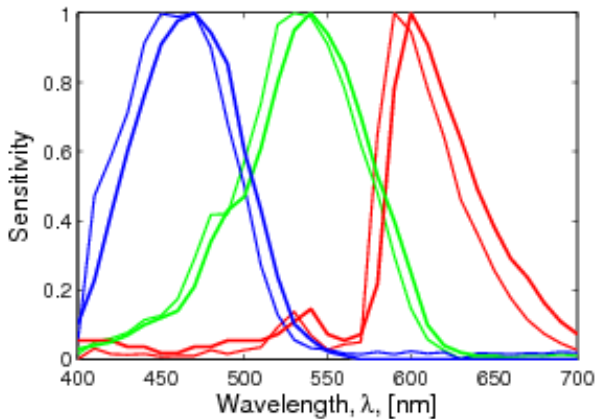


Figure 1: Camera sensitivities: Nikon D70 (thin), Canon 20D (thick)

2. *Filters*: Two hundred sixty five optical filters of three different types: exciter, dichroic, and emitter from Omega[11] are used in the simulation. Rather than mixing filters from different vendors, one vendor has been chosen as a one point solution for the filter and Omega has been picked as it has a large selection of filters and data is available online [11].

3. *Test Target*: The GretagMacbeth Color Checker DC has been used as the training target and the classic Macbeth Color Checker as the test target in the simulation. The outer surrounding gray patches and the glossy patches in the S-column of the DC chart have been omitted from the training dataset.

#### 4.1 Simulation Process

For a given pair of camera spectral sensitivities ( $s_1$  and  $s_2$ ), selected filters spectral transmittances ( $t_1$  and  $t_2$ ), and a light source spectral power distribution ( $L$ ), we simulate the output of the resulting six-channel multispectral acquisition system ( $C$ ), when capturing a given spectral reflectance ( $R$ ), as a simple linear multiplication and summation process, which can be expressed in a matrix notation as follows:

$$C = S^T \text{Diag}(L)R$$

The spectral sensitivities of the simulated six-channel multispectral system ( $S$ ) are obtained by combining sensitivity matrices of the two cameras as:

$$S = [S_1, S_2]$$

$$\text{Where } S_1 = \text{Diag}(t_1)s_1 \text{ and } S_2 = \text{Diag}(t_2)s_2$$

As there is always acquisition noise introduced into the camera outputs, to make the simulation more realistic, simulated random shot noise and quantization noise are introduced. Recent measurements of noise levels in a trichromatic camera suggest that realistic levels of shot noise are between 1% and 2% [12]. So 2% normally distributed Gaussian noise is introduced as a random shot noise in the simulation. And 12-bit quantization noise is incorporated by directly quantizing the simulated responses after the application of shot noise. Let the noisy camera response is given by  $C_n$ . The reconstructed/estimated reflectance ( $\tilde{R}$ ) is obtained for the original reflectance ( $R$ ) from the camera responses for the training and test targets using different estimation methods. Results with three popular methods, Maloney and Wandell (MW) [13], Imai and Berns (IB) [14]; and Constrained Least Square-Wiener (Wiener) [15] are investigated. The estimated reflectances with these three methods are given by the following equations:

$$\begin{aligned} \tilde{R}_{\text{MW}} &= B(E^T B)^+ C_n \\ \tilde{R}_{\text{IB}} &= B B^T R_{\text{train}} C_{n\text{train}}^+ C_n \\ \tilde{R}_{\text{Wiener}} &= R_{\text{train}} R_{\text{train}}^t E (E^t R_{\text{train}} R_{\text{train}}^t E)^{-1} C_n \end{aligned}$$

Here  $E = \text{Diag}(L)S$  and  $B$  contain the basis vectors obtained by Singular Value Decomposition (SVD) of the training reflectances  $R_{\text{train}}$ . The number of basis vectors to be used are determined by optimization of the estimation error.  $X^+$  denotes the pseudo-inverse of  $X$ . To handle ill-posed and overfitting problem in the pseudo-inverse computation, Tikhonov regularization [16] has been implemented.

The reconstructed reflectances are evaluated using spectral as well as colorimetric metrics. Most commonly used RMS (Root Mean Square) error has been used as the spectral metric and  $\Delta E_{ab}^*$  (CIELAB Color Difference) as the colorimetric metric. These metrics are given by the equations:

$$RMS = \sqrt{\frac{1}{n} \sum_{j=1}^n [\tilde{R}(\lambda_j) - R(\lambda_j)]^2}$$

$$\Delta E_{ab}^* = \sqrt{(\Delta L^*)^2 + (\Delta a^*)^2 + (\Delta b^*)^2}$$

CIE D50 illuminant and CIEXYZ 1964 are used for computation of  $\Delta E_{ab}^*$ .

We then exhaustively search for the best pair of filters, according to each of these metrics, from among the all available filters with which the multispectral system can reconstruct the original reflectances of the twenty four Macbeth color checker patches.

## 4.2 Simulation Results

The simulation has been carried out first with two times the same type of cameras Nikon D70, and then with two different types of cameras Nikon D70, and Canon 20D. The results of estimations with the proposed 6-channel multispectral camera are compared with the 3-channel systems.

1. *With two Nikon D70 Cameras:* The simulation picks different filter pairs for minimum mean RMS and for minimum  $\Delta E_{ab}^*$  depending upon the estimation method. For minimum mean RMS, Maloney and Wandell, and Imai and Berns methods select the filter pair (XF2021-XF2203), while the Least Square-Wiener method picks the filter pair (XF2021-XF3004) (Figure 3(a)). All the three methods choose the same pair of filters (XF2030-XF2014) for minimum mean  $\Delta E_{ab}^*$  (Figure 3(b)).

As an illustration, Figure 2 shows the results of the reflectance estimation with least square-Wiener method (results are similar with other methods) along with the measured reflectances of the twenty four color patches of the Macbeth color checker classic for minimum mean RMS. The filters selected by the simulation for the two cameras (left and right in order) and the metric values corresponding to the three cases are also shown in the plots. Tables 1 and 2 show statistics of estimation errors of the different methods for 3-channel and 6-channel systems respectively.

Table 1: Estimation errors (3-channel system: Nikon D70)

Method	RMS%		$\Delta E_{ab}^*$	
	Max	Mean	Max	Mean
Maloney and Wandell	9.92	3.35	6.15	1.95
Imai and Berns	10.51	3.30	8.82	2.49
Wiener	10.96	3.22	5.70	1.90

Table 2: Estimation errors (6-channel system: Two Nikon D70)

Method	For min. RMS				For min. $\Delta E_{ab}^*$			
	RMS%		$\Delta E_{ab}^*$		RMS%		$\Delta E_{ab}^*$	
	Max	Mean	Max	Mean	Max	Mean	Max	Mean
Maloney & Wandell	2.34	1.08	1.06	0.41	2.55	1.13	1.22	0.37
Imai & Berns	2.45	1.08	1.18	0.43	2.70	1.14	1.35	0.41
Wiener	2.53	1.07	1.60	0.52	2.70	1.13	1.21	0.37

The normalized effective channel sensitivities of the multispectral system corresponding to the optimal results of the two metrics are shown in Figure 4. In these plots, thin curves correspond to the modified sensitivities of the first camera and the thick curves correspond to that of the second camera.

2. *With Nikon D70 and Canon 20D Cameras:* In this case, all three estimation methods select the filter pair (XF2203-XF2021) for minimum mean RMS (Figure 3(a)) and the pair (XF2034-XF2012) for the minimum  $\Delta E_{ab}^*$  (Figure 3(c)). Tables 3 and 4 show the statistics of

estimation errors of the different methods for 3-channel and 6-channel systems respectively.

Table 3: Estimation errors (3-channel system: Canon 20D)

Method	RMS%		$\Delta E_{ab}^*$	
	Max	Mean	Max	Mean
Maloney & Wandell	7.99	2.94	12.31	3.78
Imai & Berns	8.21	2.93	13.43	3.89
Wiener	8.60	2.91	11.80	3.72

Table 4: Estimation errors (6-channel system: Nikon D70-Canon 20D)

Method	For min. RMS				For min. $\Delta E_{ab}^*$			
	RMS%		$\Delta E_{ab}^*$		RMS%		$\Delta E_{ab}^*$	
	Max	Mean	Max	Mean	Max	Mean	Max	Mean
Maloney & Wandell	2.30	1.07	1.91	0.54	2.54	1.25	1.00	0.36
Imai & Berns	2.45	1.08	1.92	0.54	2.75	1.25	1.09	0.39
Wiener	2.72	1.11	2.29	0.75	3.09	1.19	1.12	0.48

Figure 5 shows the normalized effective channel sensitivities of the multispectral system corresponding to the optimal results of the two metric.

## 5. DISCUSSION

The results are quite promising. We can see that sensitivities of the cameras are modified in a sensible way and that the dominant wavelengths are quite nicely spread out in the spectrum. This clearly shows that the use of two RGB cameras with appropriate use of filters can function well as a multispectral system. We can expect further improvement in the results with the selection from a larger set of filters from other manufacturers as well.

We have used two different evaluation metrics RMS and  $\Delta E$ . As expected, these metrics give different filter combination as the best pairs. All the estimations methods show that our proposed six channel multispectral system outperforms the 3 channel RGB systems in both cases of camera combinations by more than 2% RMS and  $2.5\Delta E_{ab}^*$  on the average. Optimizing one metric results slightly increase in the other metric values. All the three estimation methods give more or less similar results based on both the metrics.

The results we obtained are comparable to previous work on six-channel multispectral system with HDTV cameras and custom designed filters [3]. It is to be noted that our proposed system uses the normal digital cameras along with readily available filters. This makes the system simpler, cheaper and practical. By setting up the two cameras in a stereoscopic configuration, the problem of aligning the images from two cameras can be solved using stereo matching algorithms. Instead of setting up stereoscopic configurations by joining two digital cameras, a readymade stereo camera could also be used.

## 6. CONCLUSION AND PERSPECTIVES

With this study we can conclude that the use of two RGB cameras with the proper selection of a filter pair can be a practical and feasible solution for multispectral image capture. Since the digital cameras are readily available and relatively cheaper, these with appropriate filters from among readily available filters could be used as a cheaper and faster way of capturing multispectral images. The best filter pair depends on the cameras used, more specifically on the sensitivities of the two cameras and also on the evaluation metrics as well.

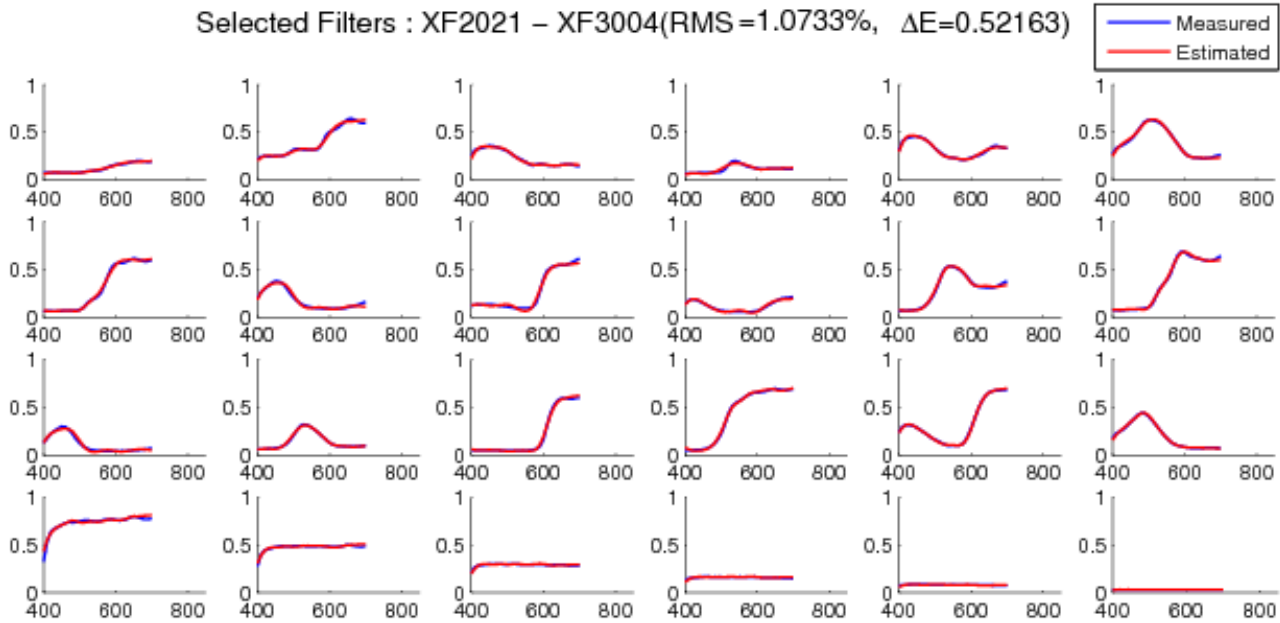


Figure 2: Reflectances with 6-channel for minimum RMS (Two Nikon D70)

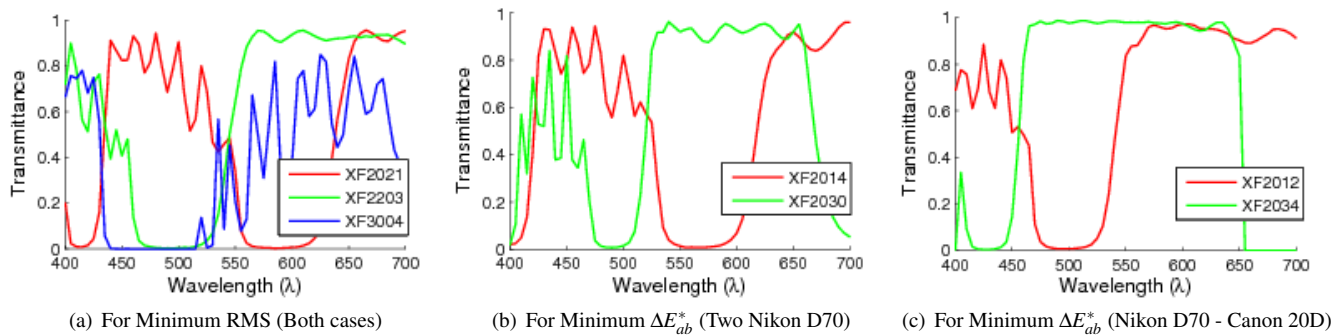
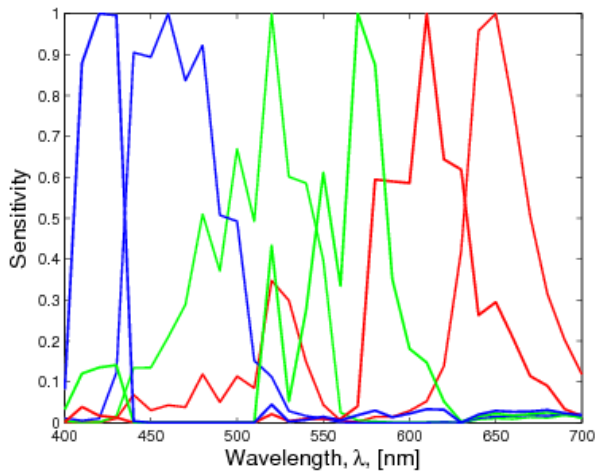


Figure 3: Transmittances of filters selected

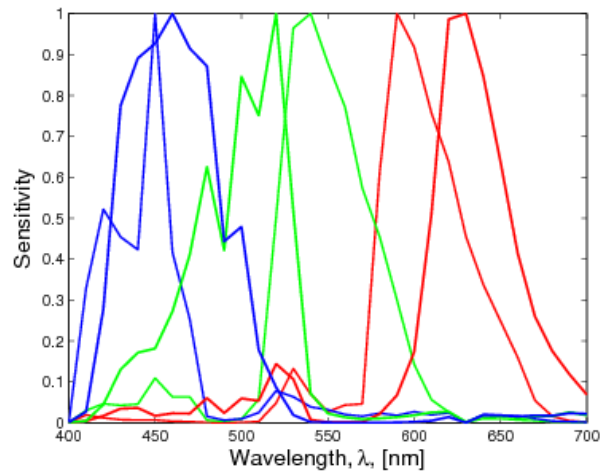
The stereoscopic configuration not only helps solve alignment problem but also provides 3D depth information along with the multispectral data. This could be an interesting further research work.

## REFERENCES

- [1] F. H. Imai, "Multispectral image acquisition and spectral reconstruction using a trichromatic digital camera system associated with absorption filters", Part VIII - General Discussion, *MCSL Technical Report*, RIT, 1998.
- [2] H. H. Huang, "Acquisition of multispectral images using digital cameras", in *The 25th Asian Conference on Remote Sensing*, 2004.
- [3] K. Ohsawa, T. Ajito, Y. Komiya, H. Fukuda, H. Hanelshi, M. Yamaguchi and N. Ohya, "Six Band HDTV Camera System for Spectrum-Based Color Reproduction," *Journal of Imaging Science and Technology*, 48(2), 85–92, 2004.
- [4] Hannah, M., "SRIs baseline stereo system," In DARPA85, 149–155, 1985.
- [5] C. Zitnick and T. Kanade, "A cooperative algorithm for stereo matching and occlusion detection," *Technical Report CMU-RI-TR-99-35*, Robotics Institute, Pittsburg, PA, 1999.
- [6] S. B. Marapane and M. M. Trivedi, "Multi-primitive hierarchical (mph) stereo analysis," *IEEE Trans. Pattern Anal. Mach. Intell.*, 16(3), 227–240, 1994.
- [7] Y.P. Hung and C. S. Chen and K. C. Hung and Y. S. Chen and C. S. Fuh, "Multipass hierarchical stereo matching for generation of digital terrain models from aerial images", *Machine Vision and Applications*, 10(5–6), 280291, 1998.
- [8] J. Y. Hardeberg, *Acquisition and reproduction of colour images: colorimetric and multispectral approaches*, Doctoral dissertation, Ecole Nationale Supérieure de Télécommunications de Paris, 2001.
- [9] J. Y. Hardeberg, "Filter selection for multispectral color image acquisition," *Journal of Imaging Science and Technology*, 48(2), 2004.

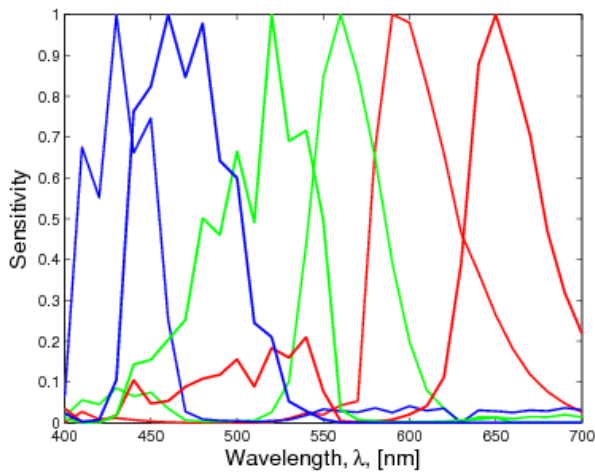


(a) For Minimum RMS

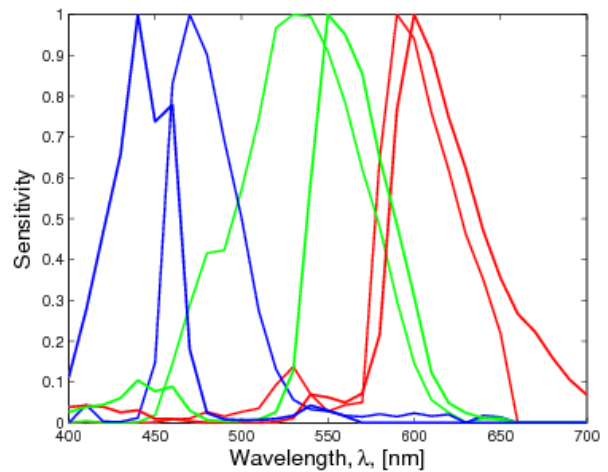


(b) For Minimum  $\Delta E_{ab}^*$

Figure 4: Multispectral 6-channel sensitivities (Two Nikon D70)



(a) For Minimum RMS



(b) For Minimum  $\Delta E_{ab}^*$

Figure 5: Multispectral 6-channel sensitivities (Nikon D70-Canon 20D)

- [10] D. C. Day, "Filter selection for spectral estimation using a trichromatic camera", M.S. Thesis, RIT, 2003.
- [11] *Omega Filters*, <https://www.omegafilters.com/curvo2/>.
- [12] K. Barnard and B. Funt, "Camera characterization for color research," *Color Research & Application*, Vol. 27, 152–163, 2002.
- [13] L. T. Maloney, *Evaluation of linear models of surface spectral reflectance with small numbers of parameters*. Jones and Bartlett Publishers, Inc., USA, 1992.
- [14] F. H. Imai and R. S. Berns, "Spectral estimation using trichromatic digital cameras." in Proceedings of *International Symposium on Multispectral Imaging and Color Reproduction for Digital Archives*, 42–49, 1999.
- [15] P. Morovic and H. Haneishi, "Estimating reflectances from multispectral video responses", in *IS&T/SID CIC14*, 131–137, 2006.

- [16] B. Dyas, "Robust sensor response characterization," in *The IS&T/SID Eighth Color Imaging Conference*, 144–148, 2000.